Biophysical Chemistry 177–178 (2013) 14–23

Contents lists available at SciVerse ScienceDirect

Biophysical Chemistry

journal homepage: http://www.elsevier.com/locate/biophyschem

Binding of new cationic porphyrin–tetrapeptide conjugates to nucleoprotein complexes

Ádám Orosz [a], Gábor Mező [b], Levente Herényi [a], Jan Habdas [c], Zsuzsa Majer [d], Beata Myśliwa-Kurdziel [e], Katalin Tóth [f], Gabriella Csík [a,*]

[a] Institute of Biophysics and Radiation Biology, Semmelweis University, 1444 Budapest POB 263, Hungary
[b] Research Group of Peptide Chemistry, Hungarian Academy of Sciences, Eötvös Loránd University, Pázmány Péter sétány 1/A, Budapest H-1117, Hungary
[c] Institute of Chemistry, University of Silesia, Katowice 40-006, Poland
[d] Laboratory of Chiroptical Structure Analysis, Institute of Chemistry, Eötvös Loránd University, Pázmány Péter sétány 1/A, Budapest H-1117 Hungary
[e] Department of Plant Physiology and Biochemistry, Jagiellonian University, ul. Gronostajowa 7, Kraków 30-387, Poland
[f] Biophysik der Makromoleküle, DKFZ, Neuenheimer Feld 280, D-69120 Heidelberg, Germany

HIGHLIGHTS

- DNA and nucleoprotein (NP) binding of porphyrin–tetrapeptide conjugates was studied with spectroscopic methods.
- Peptide conjugates of cationic porphyrins bind to DNA and NP complex
- Binding modes can be identified as intercalation and external binding.
- Probability of binding modes can be modified by the altered charge distribution and steric demands of porphyrin-conjugates

GRAPHICAL ABSTRACT

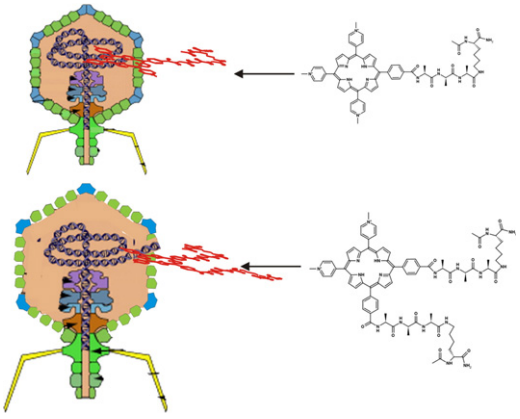

ARTICLE INFO

Article history:
Received 15 February 2013
Received in revised form 11 March 2013
Accepted 16 March 2013
Available online 2 April 2013

Keywords:
Cationic porphyrin
Porphyrin–peptide conjugate
Fluorescence spectroscopy
Induced ECD-signal
Absorption melting
Nucleoprotein–porphyrin binding

ABSTRACT

Ongoing research on DNA binding of cationic porphyrin derivatives and their conjugates is a subject of growing interest because of their possible DNA binding and demonstrated biological properties. In this study nucleoprotein binding of tri-cationic meso-tri(4-*N*-methylpyridyl)-mono-(4-carboxyphenyl)porphyrin (TMPCP) and tetrapeptides conjugated TMPCP (TMPCP-4P) and bi-cationic meso-5,10-bis(4-*N*-methylpyridyl)-15,20-di-(4-carboxyphenyl)porphyrin (BMPCP-4P$_2$) was investigated with comprehensive spectroscopic methods. The key observation is that tetrapeptide-conjugates of cationic porphyrins with two or three positive charges bind to encapsidated DNA in T7 phage nucleoprotein complex. The binding modes were analyzed by fluorescent energy transfer, fluorescent life time and CD measurements. Intercalative binding is most feasible when tricationic ligands complex with DNA, especially when it is in close connection with protein capsid. It was found that larger ligand BMPCP-4P$_2$ binds externally to encapsidated T7 DNA, and complex externally as well as by intercalation when the DNA accommodate to relaxed B-conformation. In the case of TMPCP and TMPCP-4P the intercalation is the predominant binding form both in nucleoprotein (NP) and preheated complexes. Further, melting

* Corresponding author. Tel./fax: +36 1 266 6656.
E-mail addresses: orosz.adam@med.semmelweis-univ.hu (Á. Orosz), gmezo@elte.hu (G. Mező), herenyi.levente@med.semmelweis-univ.hu (L. Herényi), jhabdas@us.edu.pl (J. Habdas), majer@chem.elte.hu (Z. Majer), b.mysliwa@wp.pl (B. Myśliwa-Kurdziel), kt@dkfz-heidelberg.de (K. Tóth), csik.gabriella@med.semmelweis-univ.hu (G. Csík).

0301-4622/$ – see front matter
http://dx.doi.org/10.1016/j.bpc.2013.03.003

experiments revealed that bound porphyrins do not influence the capsid stability or protein–DNA interactions, but efficiently stabilize the double helical structure of DNA without respect to binding form. A good correlation was found between porphyrin/base pair ration and DNA strand separation temperature.

1. Introduction

DNA is an important drug target, in particular in the treatment of cancer, where many compounds that bind covalently and/or non-covalently to DNA, or damage DNA, are used [1–5]. Cationic porphyrins like 5,10,15,20-tetra(*N*-methylpyridinium-4-yl)porphyrin (TMPyP) have historically received attention because they are water-soluble and naturally drawn to the DNA polyanion. A great number of studies deal with the interaction of cationic porphyrins with DNA as the formation of porphyrin–DNA complexes [6–11].

Recently some bioactive moieties [12–17] were introduced onto the periphery of the cationic porphyrin in order to either utilize porphyrin as DNA targeting agent or increase the cellular uptake of porphyrins. Among others, branched chain polymeric polypeptides with polylysine backbone can be considered as potential carriers of drug molecules due to their fluidic endocytosis [18].

We designed porphyrin conjugates of a tetrapeptide (Ac-Lys(H-Ala-D-Ala-Ala)-NH_2) as monomeric unit of branched polypeptide with polylysine backbone [19,20]. The N-terminus of the oligo-alanine branch was used for the attachment of the porphyrin derivatives meso-tri(4-*N*-methylpyridyl)-mono-(4-carboxyphenyl)porphyrin (TMPCP) or meso-5,10-bis(4-*N*-methylpyridyl)-15,20-di-(4-carboxyphenyl)porphyrin (BMPCP). We have reported on the interaction between natural nucleic acid polymer and tetra-peptide conjugates of TMPCP and BMPCP as models of porphyrin–peptide conjugates. Evidences provided by the decomposition of absorption spectra, fluorescence decay components, fluorescence energy transfer and induced ECD signals revealed that peptide conjugates of di- and tricationic porphyrins bind to DNA by two distinct binding modes which can be identified as intercalation and external binding. Tri-cationic structure and elimination of negative charges in the peptide conjugates are preferred for the binding [20].

Under experimental conditions (pH, ionic strength, concentration, temperature) applied in the studies described above DNA was supposed to be present in canonic B-conformation. However, under physiological conditions the conformation of DNA is rather complex, and the therapeutic target for DNA-binding agents is not the naked DNA. It is known that DNA shows remarkable flexibility in response to the application of forces and can undergo major conformational rearrangements. In nature proteins apply external forces to DNA and induce deformations on both short and long length scales [21]. Nevertheless, these conformational alterations could crucially modify the drug–DNA interactions. Considering the above observations, investigations of porphyrin–DNA interactions have to be extended to the binding of drug to nucleoprotein complexes (NP).

In cells, at the lowest level in the hierarchy DNA is wrapped around a protein complex to form nucleosome [22]. In bacteriophages the organization of the DNA by the coat protein groove and core protein structure may be similar to the manner in which DNA is ordered by wrapping about the nucleosome core [23]. In the mature head of T-like phages, the DNA is organized as a tightly wound coaxial spool, with the DNA coiled around the core [24–27]. Based on the similarities between nucleosomal and phage structure, these bacteriophages can be recommended as model systems in NP-porphyrin binding studies.

It was shown before that tetra-cationic TMPyP binds to DNA regardless of whether the polynucleotide is part of a nucleoprotein complex (nucleosome and phage NP) or not [9]. However, it is not known how the presence of proteins, e.g., viral capsid proteins or histones, influences the interaction between DNA and peptide-conjugates of cationic porphyrins. Both qualitative and quantitative characteristics of the binding can be modified by the altered charge distribution, steric requirements and conformation of peptide-conjugated porphyrins.

In the work presented here we asked the question how does the presence of protein capsid influence the binding of porphyrin-conjugates to viral DNA? The aim of this work was the qualitative and quantitative characterization of the binding of BMPCP- and TMPCP-tetrapeptide conjugates to T7 phage nucleoprotein.

We selected T7 as nucleoprotein complex for two reasons. (1) Phage nucleoprotein has been considered as a model for compact packing of DNA within chromosomes as described above. (2) Samples of both T7 phage and its isolated DNA can be prepared in optical grade purity and in sufficiently high concentration [28]. Isolated T7 DNA was used already in DNA–porphyrin-conjugates binding studies. In this way, two different conformations of the same natural polynucleotide could be investigated. We performed experiment also with T7 phage preincubated at 65 °C (NP(65 °C)). It is known that the phase transition around 60 °C results the loosening of the capsid structure and the relaxation of the DNA chain from the condensed intraphage conformation into the regular B-conformation, but the separation of protein and nucleic acid part still does not occur. In such a way a transition state between intraphage and naked DNA can be received.

2. Materials and methods

2.1. Materials

All amino acid derivatives and 4-methylbenzhydrilamine (MBHA) resin were purchased from Iris Biotech Gmbh (Marktredwitz, Germany). Coupling agents (*N*,*N*′-diisopropylcarbodiimide (DIC), 1-hydroxybenzotriazole (HOBt), (benzotriazol-1-yloxy)tris(dimethylamino)-phosphonium hexafluorophosphate (BOP), 1-ethyl-3-(3-dimethylaminopropyl)carbodiimide (EDC), *N*-ethyl-diisopropylamine (DIEA), diethylamine (DEA)), and cleavage reagents (trifluoroacetic acid (TFA), *p*-cresol, hydrogen fluoride (HF), 1,8-diazabicyclo-[5.4.0] undec-7-ene (DBU), piperidine) were Fluka products (Buchs, Switzerland). Solvents (dichloromethane (DCM), *N*,*N*-dimethylformamide (DMF), diethylether) for synthesis were obtained from Molar Chemicals (Budapest, Hungary). Acetonitrile for HPLC was delivered by Sigma-Aldrich (Budapest, Hungary).

meso-Tri(4-*N*-methylpyridyl)-mono-(4-carboxyphenyl)porphyrin (TMPCP) was synthesized as described before [29,30], and meso-5,10-bis(4-*N*-methylpyridyl)-15,20-di-(4-carboxyphenyl)porphyrin (BMPCP) was purchased from Frontier Scientific (Carnforth, UK). Porphyrins were stored at 4 °C in powder form or as a stock solution in distilled water or in methanol. Before the experiments the porphyrin stock solutions were diluted into methanol or into a buffer solution composed of 20 mM Tris–HCl and 50 mM NaCl adjusted to pH = 7.4.

2.2. T7 bacteriophage

In binding experiments T7 phage was used as nucleoprotein complex (NP). T7 (ATCC 11303-B7) was grown on *Escherichia coli* (ATCC 11303) host cells in our laboratory. The cultivation and purification

were carried out according to the method of Strauss and Sinsheimer [31]. The phage suspension was concentrated on a CsCl gradient and dialyzed against buffer solution described above. The concentration of T7 bacteriophage and base pair concentration of the samples was determined from the optical density of the samples using a molar absorptivity of $\varepsilon_{260} = 7.3 \cdot 10^3$ (mol nucleotide bases l^{-1} cm^{-1}) in phosphate buffer. In some experiments T7 phage suspension was pretreated at 65 °C for 30 min (NP(65 °C)).

2.3. Preparation of DNA from nucleoprotein complexes

DNA was prepared from nucleoprotein complexes by incubating with 0.5% SDS for 30 min at 65 °C; followed by precipitation with 1 M KCl on ice for 10 min. The precipitate was centrifuged twice for 10 min in an Eppendorf microcentrifuge at 13,000 rpm. The DNA was precipitated with ethanol from the supernatant. The pellet was washed with 70% ethanol, and resuspended in buffer solution 20 mM Tris–HCl, and 50 mM NaCl (pH = 7.4). The amount of DNA was determined spectrophotometrically. The quality of the DNA was checked by gel electrophoresis and by its absorption spectrum.

2.4. Synthesis of Ac-Lys(H-Ala-D-Ala-Ala)-NH_2

The synthesis of Ac-Lys(H-Ala-D-Ala-Ala)-NH_2 model tetrapeptide was described previously [20]. Briefly, the Ac-Lys(H-Ala-D-Ala-Ala)-NH_2 was prepared by solid phase peptide synthesis on 4-methylbenzhydrilamine resin (MBHA) using standard Boc-strategy. The peptide was cleaved from the resin with liquid hydrogen fluoride (HF) in the presence of *p*-cresol as scavenger (0.5 g/10 mL HF) at 0 °C for 1 h. The crude product was precipitated with dry ether and it was purified by RP-HPLC. The purified tetrapeptide was characterized by analytical HPLC and ESI-MS.

2.5. Conjugation of porphyrine derivatives to Ac-Lys(H-Ala-D-Ala-Ala)-NH_2

Conjugation of porphyrine derivatives was performed as it was described previously [20]. Briefly the porphyrin derivatives were attached to the tetrapeptide in DMF solution by the aid of coupling agents either BOP reagent or a water soluble carbodiimide EDC. BOP reagent was preferred to develop TMPCP conjugate, however, better yield was observed in the preparation of BMPCP conjugate when EDC was applied. One tetrapeptide was conjugated to the porphyrin derivative in case of TMPCP, while BMPCP cross-linked two tetrapeptide chains. The conjugates were purified by RP-HPLC and characterized by ESI-MS. The positively charged pyridines in porphyrin conjugates had to be taken into account for adequate explanation of the mass spectra.

2.6. Absorption spectroscopy

Ground-state absorption spectra of porphyrin and porphyrin–peptide conjugate solutions were recorded with 1 nm steps and 2 nm bandwidth by the use of a Cary 4E (Varian, Mulgrave, Australia) spectrophotometer at various NP concentrations. The composition of solutions was expressed in terms of an *r* number representing the molar ratio of DNA base pairs to porphyrin molecules.

In the applied concentration range the free porphyrins were in monomeric state. Spectral changes due to the adsorption of porphyrins on the cuvette wall were less than 5%.

2.7. Decomposition of absorption spectra

The spectral decomposition was performed for absorption spectra [$A(\lambda)$, absorbance versus wavelength] of the series of BMPCP-$4P_2$–, TMPCP–, TMPCP-4P–DNA complex solutions with various base-pair/porphyrin molar ratios (*r*). All the spectra were analyzed in the λ = 370–490 nm wavelength range.

For fitting we used the Gaussian multi-peaks fit routine from the Microcal Origin software. The error of the fit was determined as:

$$\chi^2 = \frac{\sum_{\lambda=370}^{490} \left[A(\lambda)_{\text{measured}} - A(\lambda)_{\text{calculated}}\right]^2}{\sum_{\lambda=370}^{490} A(\lambda)_{\text{measured}}}. \quad (1)$$

We did not apply the usual wavelength-frequency conversion. The maximum errors of the fitting parameters because of the absence of this conversion were not higher than 0.5 nm.

2.8. Fluorescence spectroscopy

Contact energy transfer from nucleic acid bases to bound porphyrin was measured from fluorescence excitation and emission spectra recorded between 220 and 330 nm (λ_{em} = 660 nm) and 580–780 nm (λ_{ex} = 260 nm), respectively. The porphyrin concentration was constant in the parallel samples, and the base pair/porphyrin ratio varied between 0 and 30.

2.9. Fluorescence decay measurements

Fluorescence lifetimes were measured using ISS K2 multifrequency cross-correlation phase and modulation fluorometer (ISS, Champaign, IL) equipped with a 300 W xenon lamp as an excitation source and a Pockel cell as a modulator of light intensity. Fluorescence signal was observed through a cutoff filter at wavelengths longer than 550 nm. Each measurement was performed for 10 modulation frequencies ranging from 1 to 200 MHz. The phase shift and demodulation ratio were measured in reference to the scattering solution of glycogen in water. The evaluated average random errors in the experimental data used then in the fluorescence lifetime analysis were equal to 0.2 and 0.004 for phase shift and modulation, respectively. The intensity decay data were analyzed according to a multi-exponential decay law using discrete exponential components. A nonlinear least square analysis program was delivered by ISS Company. Excitation wavelength was set to the maximum of the Soret absorption band of each porphyrin. The fluorescence lifetime of free porphyrin derivatives (c = 2 μM) was determined in Tris–HCl buffer (pH 7.4) buffer and in methanol. Lifetimes were also determined in the presence of T7 nucleoprotein complex at base pair/porphyrin ratio = 20.

2.10. Electronic circular dichroism

Electronic circular dichroism (ECD) measurements were made on a Jasco J-810 spectropolarimeter calibrated with ammonium *d*-10 camphorsulfonate at room temperature in 1 cm quartz cell. Spectra were recorded between 380 and 500 nm. ECD spectra of porphyrin derivatives and conjugates were recorded at various concentrations of DNA. In parallel samples the porphyrin concentration was constant. As baselines, the solvent reference spectra were used and were automatically subtracted from the ECD spectra of the samples. ECD band intensities were expressed in molar ellipticity / [Θ] deg × cm^2/dmol/ using the equation:

$$[\Theta] = \Theta/10 * c * l. \quad (2)$$

2.11. Optical melting measurements

Thermal denaturation curves of bacteriophage solutions were recorded by absorbance at 260 nm on a Cary 4 E spectrophotometer

(Varian, Mulgrave, Australia) equipped with a Peltier thermoregulator. The heating rate was 0.5 °C/min in the temperature range 25–98 °C. Five samples were measured in parallel using an automatic cell changer; the sixth sample holder was used to measure the temperature in an identical quartz cell filled with buffer. The cell holder was insulated to ensure that the temperature did not vary more than 0.1 °C between cells, even above 90 °C. The initial absorbance of the samples was adjusted to approximately 0.3 at 260 nm in quartz cells of 1 cm path length. The absorbance data were collected at every 0.5 °C. Data were treated using the program Origin7. The curves were normalized to the absorbance at room temperature, smoothed in five point intervals; derivative melting curves were calculated from the differences between adjacent points and once more smoothed for five points. The peak of derivative melting curve was accepted as the corresponding melting temperature (T_m).

3. Results

3.1. Decomposition of absorption spectra

Absorption spectra of porphyrin derivatives were recorded at constant porphyrin and various NP or NP(65 °C) concentrations. Fig. 1A and B shows two series of TMPCP-4P absorption spectra recorded at increasing base pair/porphyrin ratio (r) in the presence of NP and NP(65 °C), respectively. At increasing relative base pair concentration, the overall changes of the spectra can be characterized by hypochromism, red shift of the spectra and alteration of Q-band structure. Similar changes were observed in the case of TMPCP and BMPCP-4P$_2$. These spectral changes are typical for the cationic porphyrin–DNA interactions described before [9,20,32].

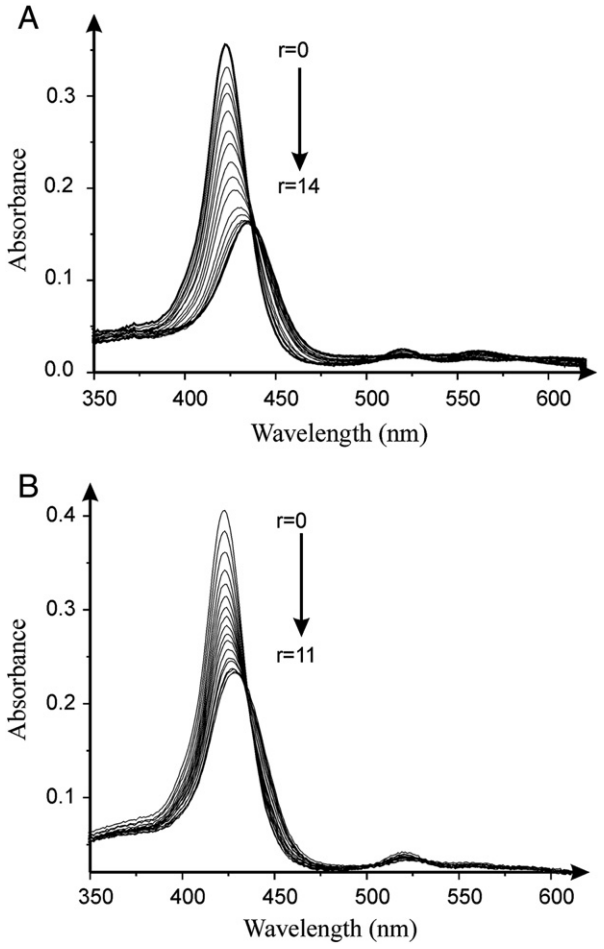

Fig. 1. Absorption spectra of TMPCP-4P at various concentrations of NP (A) or NP 65 °C (B). Base pair/porphyrin molar ratio (r) varies between 0 and 14 (A) and 0and 11 (B). Insets show the 480–610 regions of the spectra.

For further analysis of Soret bands we made assumptions as we described before [20]. Briefly, each spectrum [$A_x(\lambda)$] can be fitted as a sum of Gaussians, one of them as broad background. As a general purpose we used the least number of possible components for an acceptable fit. All the spectra could be fitted by 5 Gaussians. We kept parameters: center of the peak and full width of the band constant and the only parameter changing with the concentration of the porphyrin population in a specific state was the total area under the curves.

Fit parameters of the components of the spectra of BMPCP-4P$_2$, TMPCP and TMPCP-4P recorded in the presence of NP and NP(65°), are presented in Table 1. Higher number of component bands with than without NP suggests that out of the non-bound porphyrin molecules distinct population(s) of bound porphyrin(s) can be formed in the presence of NPs.

The relative areas under the Gaussian components (A_i^*) were determined at various base pair/porphyrin ratios (r). In Fig. 2 A_i^*-s are presented as the function r. The change in relative area of a component indicates the change of relative concentration of the corresponding porphyrin population.

In the case of BMPCP-4P$_2$ (Fig. 2A and D), component bands of the free porphyrin A_1^* ($\lambda_1 = 410$ nm), A_2^* ($\lambda_2 = 418$ nm), and A_3^* ($\lambda_3 = 421/422$ nm) are decreased by the increasing base pair/porphyrin ratios (r). Parallel to that the relative area of the only new band (A_4^* ($\lambda_4 = 426/427$ nm)) increases. These changes reflect the reduction of free porphyrin and elevation of bound porphyrin concentration with increasing r. The number of Gaussian spectral components suggests the formation of a single population of bound porphyrin; the position of new spectral band – about 5 nm red-shift as compared to the free porphyrin – makes likely that the binding form is external binding.

In the case of TMPCP and TMPCP-4P a new band centered around 434/435 nm and increasing with NP concentration can be clearly recognized. This about 10 nm spectral shift is typical for the intercalation of porphyrin moiety.

The changes of the spectral bands located around 426–429 nm require further considerations. This band is present in the spectra of free TMPCP and TMPCP-4P and also in bound ones both in the presence of NP and NP(65°). However the spectral area (A^*) changes in the function r are not uniform (see Fig. 2B and E). As it was shown above, in the case of BMPCP-4P$_2$ this is the only band which becomes more dominant due to the binding.

In TMPCP–NP(65°) binding contribution of this band clearly increases; in TMPCP-4P–NP/NP(65°) interactions it decreases, but the rate of the change varies with the specific interactions. It cannot be excluded that this spectral range covers two unresolved bands: one belonging to the free porphyrins and one band of a bound forms overlapping with each other. The increase of the number of component bands may separate two neighboring bands in the region in question, but parallel to that the inaccuracy of the fitting also increases (data not shown).

Table 1
Fitted parameters of the components of Soret bands (370–490 nm) in Tris–HCl buffer (pH 7.4): λ_i (nm) is the center of the peaks, and w_i (nm) is the full width of the bands received in the presence of NP and NP(65°). Errors are less than 1 nm for λ_i, and less than 0.5 nm for w_i.

Compounds		λ_1	w_1	λ_2	w_2	λ_3	w_3	λ_4	w_4
BMPCP-4P$_2$	NP	410	23	418	9	422	14	426	23
	NP(65°)	410	21	418	8	421	15	427	20
TMPCP	NP	401	16	421	17	429	25	434	30
	NP(65°)	401	14	421	19	429	26	444	24
TMPCP-4P	NP	403	15	422	16	427	25	435	27
	NP(65°)	403	16	422	16	427	27	435	29

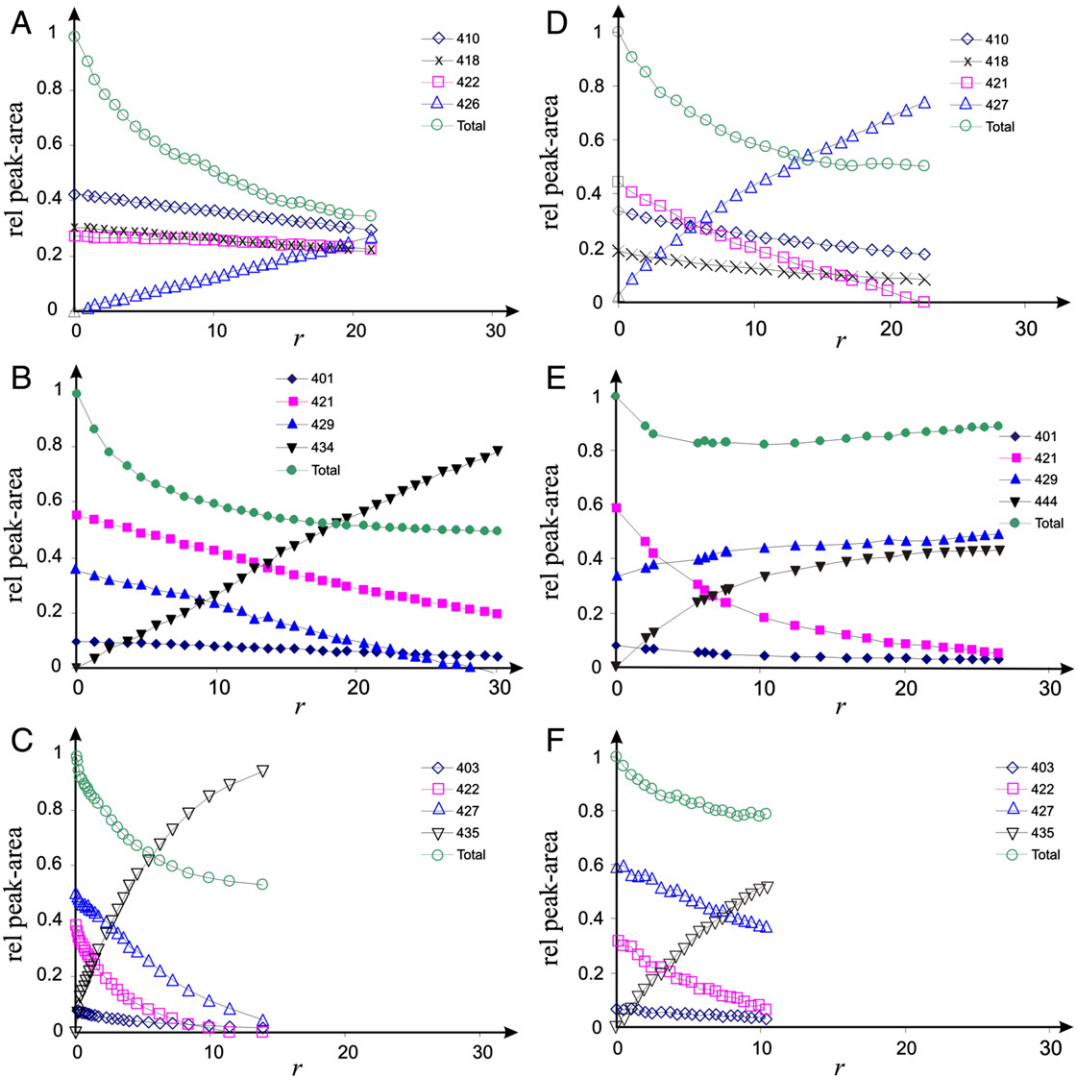

Fig. 2. Relative area of the components of the absorption spectra of BMPCP-4P$_2$ (A and D), TMPCP (Band E) and TMPCP-4P (C and F) in the presence of T7 NP (A–C) or NP(65 °C) (D–F) as a function of base pair/porphyrin molar ratio (r) in DNA. Absorption bands are identified by the position of corresponding maxima indicated in the Figure.

In summary we can conclude that decomposition of the absorption spectra proves the presence of at least one binding form for each investigated porphyrin derivatives. Beyond that, our results do not exclude the possibility of a second binding form in between TMPCP or TMPCP-4P and components of NPs.

Significant differences can be recognized also between the binding ability of the investigated compounds which varies also with the partners of the interactions. Gaussian components of free TMPCP-4P spectrum become negligible at about $r = 10$. In all the other cases higher base pair/porphyrin ratio is needed for the saturation of the binding process, but this ration is typically lower in the case of NP(65°) bindings than in NP bindings.

3.2. Fluorescence decay measurements

As a very sensitive signal of the changes of chromophore's environment, the fluorescence lifetime of porphyrins and porphyrin–peptide conjugates was measured at room temperature. The lifetimes of fluorescent porphyrin species obtained at $r = 20$ are presented in Table 2.

In the case of BMPCP-4P$_2$ a single exponential decay was observed in the presence of NP and two exponential decay in the presence NP(65°). In all the other cases the best fit was achieved by a bi-exponential function. The longer lifetime components are in the range of 9.7–10.5 ns, and the shorter ones between 2.3 and 3.5 ns. For TMPCP and TMPCP-4P these values are clearly different from the lifetime of free species, 4.2 and 4.9 ns, respectively. These results show that two populations of bound TMPCP and TMPCP-4P can be formed in the presence of NP or NP(65°). The received lifetime ranges are in good agreement with the lifetimes of intercalated and externally bound tetra-cationic porphyrin determined by Shen et al. [33]. From these similarities, one can suppose that both intercalated and externally bound porphyrins are present here.

Table 2
Fluorescence lifetimes (τ) (ns) of porphyrin derivatives and peptide conjugates in Tris buffer (pH = 7) in the presence of T7 NP and NP(65 °C).

Compounds		τ_1	τ_2
BMPCP-4P$_2$	NP	–	9.14
	NP (65 °C)	3.08	10.25
TMPCP	NP	3.14	10.56
	NP (65 °C)	3.52	10.1
TMPCP-4P	NP	3.13	9.87
	NP (65 °C)	3.19	9.74

3.3. Fluorescence energy transfer

Fluorescence-energy transfer experiments provide complementary information about the binding mode of a dye with DNA [34].

We recorded the fluorescence emission spectra of porphyrin–NP samples between λ = 580 and 800 nm when they were excited at λ = 260 nm. Fig. 3A and B shows the relative integrated fluorescence intensity (I_{rel}) of porphyrin derivatives (1 μM) at various concentrations of T7 NP (4A) or preheated NP (4B). Since the fluorescence intensity of free porphyrins in the 580–800 nm wavelength range upon excitation at λ = 260 nm is not zero (see also Fig. 4), the references were the fluorescence intensities of corresponding NP-free samples.

A significant increase in the emitted intensity can be observed at constant porphyrin and increasing base pair concentration in the case of TMPCP and TMPCP-4P when NP or NP(65°) is added to the samples. In the presence NP or NP(65°) BMPCP-4P2 shows non or much smaller increase in its fluorescence signal then the other two compounds.

The saturation of the process can be reached at different base pair/porphyrin molar ratios depending on both the type of the porphyrin and the higher order structure of the nucleic acid. It is a general tendency that the lowest base pair excess for the saturation is required when the nucleic acid is present in isolated form [20] and the highest one for the intact NP.

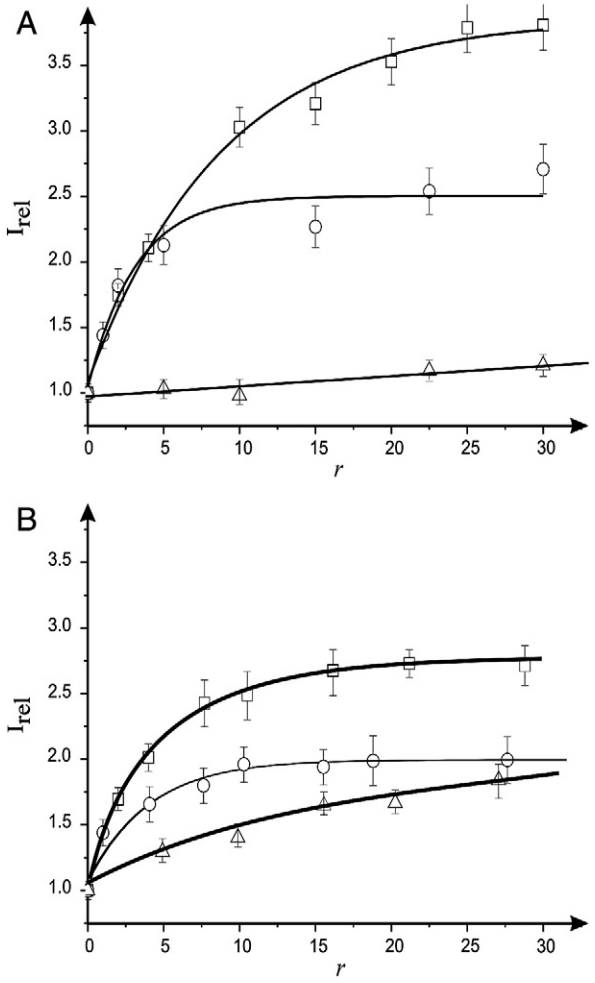

Fig. 3. (A) Integrated relative fluorescence intensity of TMPCP (open square), TMPCP-4P (open circle), and BMPCP-4P_2 (open triangle) upon excitation at λ = 260 nm as the function of the NP (A) or NP(65 °C) (B) base pair/porphyrin molar ratio (r). The concentration of porphyrin was 1 μM.

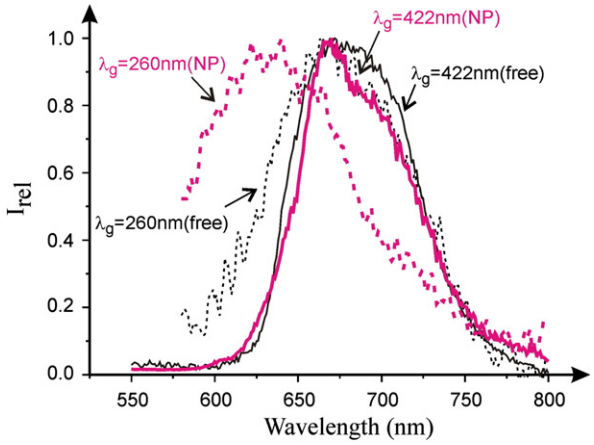

Fig. 4. Normalized fluorescence emission spectra of TMPCP-4P upon excitation at λ = 260 nm (dashed lines) or λ = 422 nm (solid lines) without (thin lines) and with NP (bold lines). Base pair/porphyrin molar ratio was about 10.

Out of the increased fluorescence intensity in the presence of DNA or NP, the altered shape of emission spectrum upon 260 nm excitation can be indicative of energy transfer.

In Fig. 4 normalized fluorescence emission spectra of TMPCP-4P upon excitation at λ = 422 nm (spectra 1 and 2) and λ = 260 nm (spectra 3 and 4) without (spectra 1 and 3) and with NP (spectra 2 and 4) are presented. The spectrum of free TMPCP-4P received at 260 nm excitation can be characterized by a broad emission band centered around 675 nm that is blue shifted by about 40 nm when it is recorded in the presence of NP at r = 10 (spectrum 4). Value of the shift of the emission band was a function of base pair/porphyrin ratio (data not shown). This can be interpreted as the higher contribution of DNA-bound molecules to the allover fluorescence of TMPCP-4P at increasing r values.

Similar spectral shift was detected due to the interaction of TMPCP-4P with NP(65°), and also for TMPCP in the presence of NPs (data not shown).

3.4. Electronic circular dichroism

In addition to absorption spectra and energy transfer measurements, ECD study is a useful tool for the diagnostic of the interaction of cationic porphyrins with DNA or NP complex [32,35–37]. All the three compounds, BMPCP-4P_2, TMPCP and TMPCP-4P display induced ECD spectrum in the presence of NP and NP(65 °C) at r = 20, as it is demonstrated in Fig. 5. The addition of T7 NP to BMPCP-4P_2 induces a single positive band around 420 nm. In all the other cases presented in Fig. 5A and B, ECD spectra composed of a positive and a negative band can be detected. Positive bands are centered on λ = 425 nm (TMPCP and TMPCP-4P), and negative ones are centered around 437 and 445 for BMPCP-4P_2 and TMPCP, TMPCP-4P, respectively.

The relative intensity of spectral bands varies according to the type of the porphyrin. In the case TMPCP and TMPCP-4P the positive bands exhibit smaller intensity than the negative bands both in the compact and loosened phage structure. This can reflect on the relative dominancy of different binding types.

Induced ECD signals were more intense with increasing base pair/porphyrin ratio (data not shown). The base pair/porphyrin ratios leading to the apparent saturation of the binding process vary with the structure of compound.

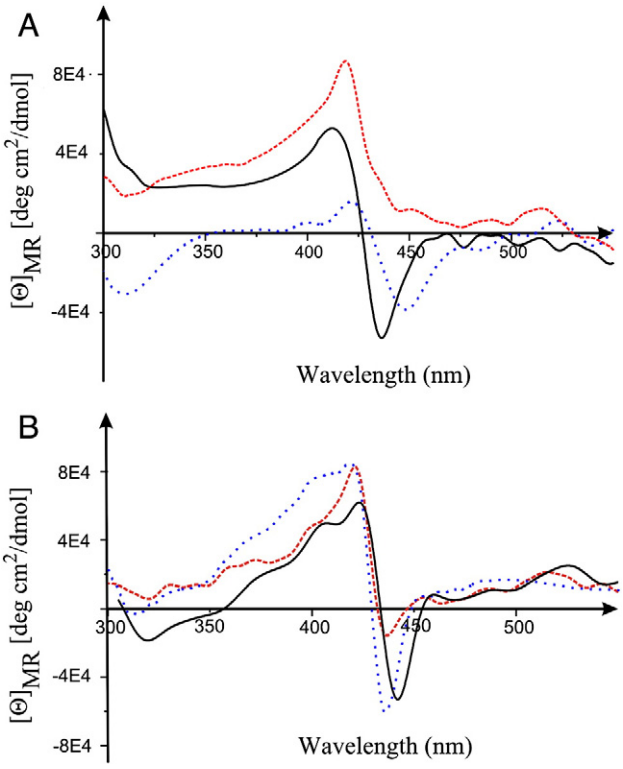

Fig. 5. ECD spectra of BMPCP-4P$_2$, (dashed line) TMPCP (solid line)and TMPCP-4P (dotted line), in the presence of T7 NP (A) or NP(65 °C) (B) at $r = 30$. The concentration of porphyrin was 1 μM.

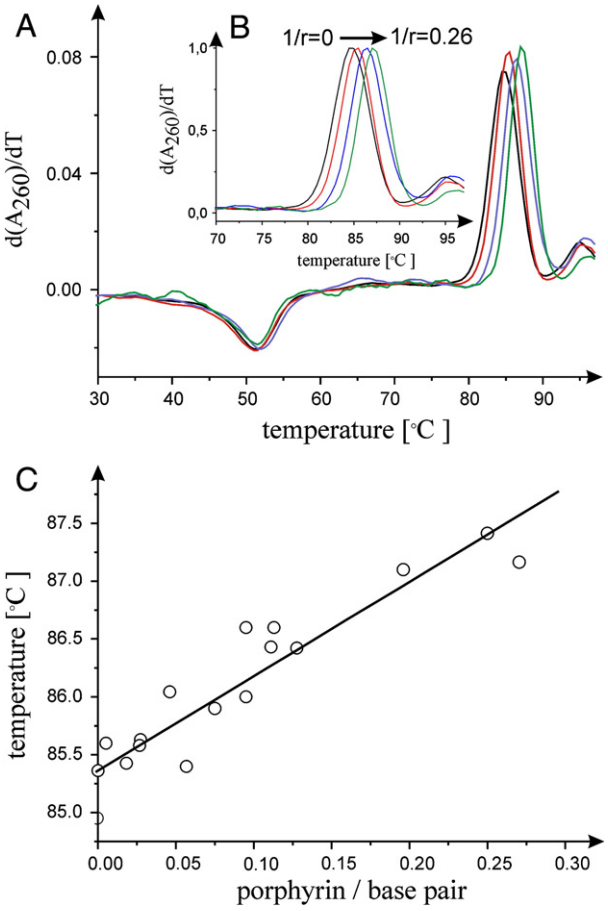

Fig. 6. (A) Derivative melting curves of T7 NP in the presence of TMPCP-4P. (B) Normalized derivative melting curves of T7 NP in the 70–100 °C range in the presence of TMPCP-4P. Porphyrin/base pair ratios ($1/r$) are: 0 (black), 0.06 (red) 0.11 (purple) and 0.26 (green). (C) Melting temperature of T7 NP as the function of the porphyrin/base pair ratios. Line was fitted by linear regression (correlation coefficient = 0929).

3.5. Optical melting measurements

The interaction between porphyrin derivatives and DNA or NP complex can lead to the stability changes in macromolecules. To look for possible structural changes caused by the porphyrin binding, the thermal stability of T7 phage and DNA was detected by optical melting method, i.e., the thermal denaturation of the whole T7 phage and isolated DNA was monitored via the changes in their absorbance at 260 nm.

As an example, the melting derivative curves of T7 NP recorded at various TMPCP-4P and constant base pair concentrations are presented in panel A of Fig. 6. In panel B the normalized form of the curves presented in panel A is shown in the temperature range 70–98 °C.

All curves in Fig. 6A show the two structural transitions typical for T7 nucleoprotein complex: a hypochromic change between 50 and 60 °C and a hyperchromic one around 85 °C [38]. The low-temperature transition is due to the disruption of the phage capsid. During this transition, the DNA is partly released from the capsid, it relaxes to a regular B tertiary structure and loses its higher order arrangement. The hyperchromic transition around 85 °C is attributed to the denaturation of the DNA double helix: the opening of the H bonds, weakening of the stacking interaction and the separation of the two single strands. In a melting derivative curve of isolated DNA only the hyperchromic transition is present around 85 °C [38].

It can be seen in Fig. 6A that up to 0.5 porphyrin/base pair molar ratios ($1/r$) the melting parameters of phage capsid disruption remain unchanged; that is, the presence of this compound does not influence the stability of phage protein capsid and/or DNA–protein interaction.

In the same concentration range of TMPCP-4P the melting temperature of DNA strand separation is shifted to the higher values as the concentration of porphyrin conjugate increases (Fig. 6A and B). Similar changes were induced in the case of isolated DNA (data not shown). This means that both isolated and encapsulated DNA can interact with the porphyrin-conjugate and the binding results in the stabilization of DNA structure.

The presentation of the main phase transition temperature as the function of porphyrin/base pair ratio not only shows the stabilizing effect of the compounds but also facilitates the comparison of their efficacy with each other and in their reactions with DNA and NPs. Fig. 6C presents this function for TMPCP-4P; the other data: slopes of the fitted lines and correlation coefficients are summarized in Table 3.

Table 3
Slopes of the porphyrin/base pair ratio–helix/coli transition melting temperature functions (see Fig. 6C) and (in brackets) the correlation coefficients of linear fits. Melting temperatures of isolated T7 DNA (DNA), T7 phage (NP) and T7 incubated at 65 °C before porphyrin interaction (NP(65 °C)) were measured in the presence of porphyrins and porphyrin conjugates. Porphyrin/base pair ratio was varied between 0 and 0.5. DNA or NP concentration was around $5 * 10^{-5}$ M.

Compounds	DNA	NP	NP(65 °C)
BMPCP-4P$_2$	22.72 (0.873)	3.3 (0.745)	8.48 (0.816)
TMPCP	20.46 (0.935)	8.15 (0.929)	10.99 (0.985)
TMPCP-4P	80.58 (0.985)	30.4 (0.993)	27.09 (0.939)

TMPCP-4P proved to be the most effective in DNA stabilization, i.e., it has the highest slope of $(1/r) \rightarrow T$ functions. TMPCP and BMPCP-4P_2 have almost similar stabilizing effect when they bind to free DNA. Data shows that probably TMPCP has an easier access to encapsulated DNA than BMPCP-4P_2. Also, similar porphyrin concentration causes always higher temperature shift in free than in intra-phage DNA or in loosened phage structure of NP(65°).

4. Discussion

Cationic porphyrins are of great interest as they are able to bind to macromolecules, specifically to nucleic acids. Recently cationic porphyrin–peptide conjugates were synthesized to enhance the cellular uptake of porphyrins [39,40] or deliver the peptide moiety to the close vicinity of nucleic acids [41,42].

As an initial step in the study of the DNA binding ability of porphyrin–peptide conjugate we synthesized two new porphyrin–tetrapeptide conjugates which can be considered as a typical monomer unit corresponding to the branches of porphyrin-polymeric branched chain polypeptide conjugates. We investigated the complex formation between the di- and tri-cationic porphyrins and their tetrapeptide-conjugates and isolated DNA of T7 bacteriophage.

It was shown that peptide conjugates of di- and tricationic porphyrins bind to free DNA by two distinct binding modes which can be identified as intercalation and external binding [20]. However, the therapeutic targets for DNA-binding agents are nucleoprotein complexes and not the naked DNA, and the presence of proteins can critically influence DNA accessibility to the binding agents. Here we investigated the binding of tricationic porphyrin derivative (TMPCP), and peptide conjugates of di- and tri-cationic porphyrins (BMPCP-4P_2 and TMPCP-4P) to nucleoprotein complex with comprehensive spectroscopic methods.

Results of absorption spectroscopy i.e., NP concentration dependent red shift and hypochromicity of absorption spectra (Fig. 1) prove the interaction between porphyrin-conjugates and NPs. Similar spectral changes were observed before at increasing concentration of naked T7 DNA. However, decomposition of the absorption spectra of a porphyrin derivative recorded in the presence of DNA or NP leads to different results.

When DNA was added to the porphyrin or porphyrin–peptide conjugate solutions the amplitudes of two component absorption bands were increasing, and the amplitude of the main band of free porphyrins were diminished with increasing base pair/porphyrin ratio. One of the increasing amplitude was centered around 429 nm for all the investigated compounds. The centers of the other new bends were 446 and 435 nm in the case of tri-and di-cationic compounds, respectively.

Among the components of absorption spectra of porphyrin–NP complexes we can recognize one component which is not present in the case of free porphyrins. This new band is at 426 nm in the case of BMPCP-4P_2 and at 434/435 nm for TMPCP and TMPCP-4P. Comparing this result with the position of component bands received for the porphyrin–DNA complexes [20] and with the position of the absorption bands of intercalated and externally bound forms determined before for other cationic porphyrin–DNA complexes [43] we can conclude that the 426 nm is indicative for the groove-binding and the 434/435 nm could indicate the intercalated form of porphyrin derivative. Neither of porphyrin–NP complexes presents such spectral band which is not present in the case of porphyrin–DNA complexes [20] and can be assigned to the interaction between porphyrin and protein capsid around the nucleic acid. These conclusions are valid also for porphyrin–NP(65°) complexes, however there are differences in the relative contribution of the distinguished spectral bands to the allover absorption.

In the identification of binding modes of porphyrins energy transfer measurements and CD spectroscopy can serve further information. Since the first report of contact energy transfer from DNA bases to bound ligands by Le Pecq and Paoletti [44], this technique has been used frequently in DNA–ligand interaction studies. Porphyrins that contact closely with DNA bases are characterized by a clear increase of their fluorescence quantum yields for an excitation around 260 nm, corresponding to an energy transfer from DNA bases to porphyrins. This phenomenon was considered by several authors as a criterion for intercalation [45,46]. However, it was shown by Hyan et al. that DNA bases can transfer excited energy to bound ligands even though the binding mode is not intercalative but porphyrin is bound in the minor groove [47].

With the exception of BMPCP-4P_2–NP complex, the increased fluorescence intensity of porphyrins in porphyrin–NP complexes can be detected. Thus, the observation of efficient energy transfer from a host DNA to a bound TMPCP and TMPCP-4P suggests that these compounds are in close vicinity of DNA bases.

It was demonstrated before that the appearance of a negative induced ECD band is a signature for intercalation whereas a positive induced band is indicative of a non-intercalated binding mode [35,48,49]. In contrast, remarkable induced CD signal of cationic porphyrins in the presence of proteins was not reported [50].

Our presented observations support the view that all the three derivatives go to complex formation with NP and NP(65 °C). Based on the characteristics of ECD spectra we can suppose that intercalated and externally bound porphyrin forms could be present both in TMPCP– and TMPCP-4P–NP complexes, moreover in BMPCP-4P_2–NP(65 °C) as well. In BMPCP-4P_2–NP complexes only externally bound porphyrins are shown by ECD spectra.

Fluorescence lifetime measurements provided additional insight into the interaction between porphyrins and NPs. When fluorescence decay of BMPCP-4P_2 was followed in the presence of NP at $r = 20$ the best fit was achieved by a one-exponential function. That is, the lifetime identifies a single binding form under these conditions. In all the other cases for all the three compounds both in the presence of NP or NP(65 °C) the best fits were received by bi-exponential functions from which one is shorter and the other is longer than the lifetime of free porphyrins. These values are typical for the intercalated and externally bound forms of cationic porphyrins [9] and are in good agreement with the lifetimes determined for the same derivatives in their DNA-complexes [20]. Based on these conformabilities we could identify the shorter lifetimes as belonging to intercalated species, the longer ones as belonging to externally bound forms.

Both the fluorescence decay and the ECD measurements prove that in the complexes of NPs and three-cationic TMPCP and its peptide-conjugate two binding forms can be distinguished, likewise in BMPCP-4P_2–NP(65 °C) complex.

Also these results point out the limits of information provided by spectral decomposition. Analysis of absorption component spectra clearly showed the interaction between porphyrin derivatives and NPs, and the differences between two- and three-cationic compounds were also indicated. However, the overlapping of spectral bands or the small amplitude of the absorption of certain porphyrin populations did not facilitate the convincing separation of binding forms.

Stability changes of target structures can also reflect on the drug-target interactions. Thermal denaturation of DNA and nucleoproteins is one of the most frequently used physical methods for studying the stability changes of a nucleic acids and nucleoprotein complex [51,52]. Here we observed that the DNA strand separation temperature was gradually increased as the function of porphyrin/base pair ratio meanwhile the first phase transition temperature remains constant. This means that the thermal stability protein structure was not influenced by the presence of porphyrin derivatives.

It was shown before that both intercalation and groove binding of porphyrin species result in the elevation of DNA melting temperature [53–55]. Moreover the melting temperature of the DNA was observed to increase in direct proportion to the number of occupied intercalation

sites [56]. The increase of DNA strand separation temperature in the presence of BMPCP-4P$_2$, TMPCP and TMPCP-4P both in isolated and encapsidated DNA reflects binding of these porphyrin derivatives. The order of the slopes of base pair/porphyrin–melting temperature functions: NP < NP(65 °C) < DNA corresponds to the relative accessibility of DNA (see Table 3). The correlation coefficients suggest the dominancy of intercalation as the binding forma in TMPCP and TMPCP-4P complexation processes.

We can conclude that the balance between electrostatic forces and steric requirements involved in binding process; these effects and accessibility of DNA shape together the binding motif. The protein capsid and the compact structure of encapsidated DNA in T7 nucleoprotein modify but do not inhibit the interaction between DNA and tetrapeptide-conjugates of tri- and dicationic porphyrins. Intercalative binding could be most feasible when tri-cationic ligands complex with DNA, especially when it is in close connection with protein capsid. Similar observation was published by K. Andrews and D. R. McMillin [57]. On the other hand, larger ligand BMPCP-4P$_2$ binds externally to encapsidated T7 DNA, and complex externally as well as by intercalation when the DNA accommodate to relaxed B-conformation. This view is supported also by the results of Wu and co-workers [58] showing that steric forces destabilize the intercalated form of a bulky porphyrins.

Interaction between porphyrin derivatives and phage proteins was not indicated by our results.

Acknowledgments

This work was supported by research grant OTKA NK77485, OTKA K 104045, OTKA K 100720 and MTA-DAAD project 29225. We are very grateful to Monika Drabbant for her technical assistance.

References

[1] L.H. Hurley, DNA and its associated processes as targets for cancer therapy, Nature Reviews. Cancer 2 (2002) 188–200.
[2] K. Barabas, R. Milner, D. Lurie, C. Adin, Cisplatin: a review of toxicities and therapeutic applications, Veterinary and Comparative Oncology 6 (2008) 1–18, (2008).
[3] R. Palchaudhuri, P.J. Hergenrother, DNA as a target for anticancer compounds: methods to determine the mode of binding and the mechanism of action, Current Opinion in Biotechnology 18 (2007) 497–503.
[4] C.A. Robertson, D. Hawkins, E.H. Abrahamse, Photodynamic therapy (PDT): a short review on cellular mechanisms and cancer research applications for PDT, Journal of Photochemistry and Photobiology B: Biology 96 (2009) 1–8.
[5] W.A. Denny, Synthetic DNA-targeted chemotherapeutic agents and related tumor-activated prodrugs, in: D.J. Abraham (Ed.), Burger's Medicinal Chemistry, Drug Discovery and Development, Wiley-Interscience, Hoboken, NJ, 2010, pp. 83–150.
[6] R.F. Pasternack, E.J. Gibbs, J.J. Villafranca, Interactions of porphyrins with nucleic acids, Biochemistry 22 (1983) 2406–2414.
[7] R.F. Pasternack, C. Bustamante, P.J. Collings, A. Giannetto, E.J. Gibbs, Porphyrin assemblies on DNA as studied by a resonance light-scattering technique, Journal of the American Chemical Society 115 (1993) 5393–5399.
[8] X. Shui, M.E. Peek, L.A. Lipscomb, Q. Gao, C. Ogata, B.P. Roques, C. Garbay-Jaureguiberry, A.P. Wilkinson, L.D. Williams, Effects of cationic charge on three-dimensional structures of intercalative complexes: structure of a bis-intercalated DNA complex solved by MAD phasing (Review), Current Medicinal Chemistry 7 (2000) 59–71.
[9] K. Zupan, L. Herenyi, K. Toth, Z. Majer, G. Csik, Binding of cationic porphyrin to isolated and encapsidated viral DNA analyzed by comprehensive spectroscopic methods, Biochemistry 43 (2004) 9151–9159.
[10] A. D'Urso, A. Mammana, M. Balaz, A.E. Holmes, N. Berova, R. Lauceri, R. Purrello, Interactions of a tetraanionic porphyrin with DNA: from a Z-DNA sensor to a versatile supramolecular device, Journal of the American Chemical Society 131 (2009) 2046–2047.
[11] L. Gong, I. Bae, S.K. Kim, Effect of axial ligand on the binding mode of M- meso -tetrakis(N -methylpyridinium-4-yl)porphyrin to DNA probed by circular and linear dichroism spectroscopies, The Journal of Physical Chemistry. B 116 (2012) 12510–12521.
[12] I. Dubey, G. Pratviel, B. Meunier, Preparation of cationic non-metallated or zinc-porphyrin-oligonucleotide fluorescent conjugates | [Préparation de molécules conjuguées oligonucléotide-porphyrine cationique fluorescentes non métallées ou métallées par du zinc], Comptes Rendus de l'Academie des Sciences - Series IIc: Chemistry 1 (1998) 259–267.
[13] T. Ji, Z.-X. Jiang, K. Wang, Z.-Y. Li, Binding and photocleavage of cationic porphyrin-phenylpiperazine hybrids to DNA, Biophysical Chemistry 119 (2006) 295–302.
[14] J.N. Silva, A. Galmiche, J.P.C. Tomé, A. Boullier, M.G.P.M.S. Neves, E.M.P. Silva, J.-C. Capiod, J.A.S. Cavaleiro, R. Santus, J.-C. Mazière, P. Filipe, P. Morlière, Chain-dependent photocytotoxicity of tricationic porphyrin conjugates and related mechanisms of cell death in proliferating human skin keratinocytes, Biochemical Pharmacology 80 (2010) 1373–1385.
[15] K. Steenkeste, F. Tfibel, M. Perrée-Fauvet, R. Briandet, M.-P. Fontaine-Aupart, Tracking the photosensitizing antibacterial activity of mono(acridyl)bis(arginyl) porphyrin (MABAP) by time-resolved spectroscopy, Journal of Physical Chemistry A 114 (2010) 3334–3339.
[16] L. Veverková, K. Záruba, J. Koukolová, V. Král, Oxoanion binding: a change of selectivity for porphyrin–alkaloid conjugates as a result of substitution pattern, New Journal of Chemistry 34 (2010) 117–122.
[17] A. Maraval, S. Franco, C. Vialas, G. Pratviel, M.A. Blasco, B. Meunier, Porphyrin–aminoquinoline conjugates as telomerase inhibitors, Organic and Biomolecular Chemistry 1 (2003) 921–927.
[18] F. Hudecz, Design of synthetic branched-chain polypeptides as carriers for bioactive molecules, Anti-Cancer Drugs 6 (1995) 171–193.
[19] F. Hudecz, M. Szekerke, Investigation of drug-protein interactions and the drug-carrier concept by the use of branched polypeptides as model systems. Synthesis and characterization of the model peptides, Collect. Czech, Chemical Communications 45 (1980) 933–940.
[20] G. Mező, L. Herényi, J. Habdas, Z. Majer, B. Myśliwa-Kurdziel, K. Tóth, G. Csík, Syntheses and DNA binding of new cationic porphyrin–tetrapeptide conjugates, Biophysical Chemistry 155 (2011) 36–44.
[21] C. Prévost, M. Takahashi, R. Lavery, Deforming DNA: from physics to biology, ChemPhysChem 10 (2009) 1399–1404.
[22] H.G. Garcia, P. Grayson, L. Han, M. Inamdar, J. Kondev, Ph.C. Nelson, R. Phillips, J. Widom, P.A. Wiggins, Biological consequences of tightly bent DNA: the other life of a macromolecular celebrity, Biopolymers 85 (2007) 115–130.
[23] K. Luger, A.W. Mader, R.K. Richmond, D.F. Sargent, T.J. Richmond, Crystal structure of the nucleosome core particle at 2.8 Å resolution, Nature 389 (1997) 251–260.
[24] J.E. Johnson, W. Chiu, DNA packaging and delivery machines in tailed bacteriophages, Current Opinion in Structural Biology 17 (2007) 237–243.
[25] M.E. Cerritelli, N. Cheng, A.H. Rosenberg, C.E. McPherson, F.P. Booy, A.C. Steven, Encapsidated conformation of bacteriophage T7 DNA, Cell 91 (1997) 271–280.
[26] M.E. Cerritelli, J.F. Conway, N. Cheng, B.L. Trus, A.C. Steven, Molecular mechanisms in bacteriophage T7 procapsid assembly, maturation, and DNA containment, Advances in Protein Chemistry 64 (2003) 301–323.
[27] R. Häuser, S. Blasche, T. Dokland, E. Haggård-Ljungquist, A. von Brunn, M. Salas, S. Casjens, I. Molineux, P. Uetz, Bacteriophage protein–protein interactions, Advances in Virus Research 83 (2012) 219–298.
[28] M. Hegedus, K. Modos, G. Ronto, A. Fekete, Validation of phage T7 biological dosimeter by quantitative polymerase chain reaction using short and long segments of phage T7 DNA, Photochemistry and Photobiology 78 (2003) 213–219.
[29] J. Habdas, B. Boduszek, Synthesis of new porphyrin-containing peptidyl phosphonates, Phosphorus, Sulfur, and Silicon 180 (2005) 2039–2045.
[30] J. Habdas, B. Boduszek, Synthesis of 5-(4′-carboxyphenyl)-10,15,20-tris-(4 pyridyl)-porphyrin and its peptidyl phosphonate derivatives, Journal of Peptide Science 15 (2009) 305–311.
[31] J.H. Strauss, R.L.J. Sinsheimer, Purification and properties of bacteriophage MS2 and of its ribonucleic acids, Molecular Biology 7 (1963) 43–48.
[32] M.A. Sari, J.P. Battioni, D. Dupre, D. Mansuy, J.B. Le-Pecq, Interaction of cationic porphyrins with DNA: importance of the number and position of the charges and minimum structural requirements for intercalation, Biochemistry 29 (1990) 4205–4215.
[33] Y. Shen, P. Myslinski, T. Treszczanovicz, Y. Liu, J.A. Koningstein, Picosecond laser-induced fluorescence polarization studies of mitoxantrone and tetrakisporphine/DNA complexes, Journal of Physical Chemistry 96 (1992) 7782–7787.
[34] G. Viola, H. Ihmels, H. Kraußer, D. Vedaldi, F. Dall'Acqua, DNA-binding and DNA-photocleavaging properties of 12a,14adiazoniapentaphene, ARKIVOC V (2004) 219–230.
[35] S. Lee, S.H. Jeon, B.-J. Kim, S.W. Han, H.G. Jang, S.K. Kim, Classification of CD and absorption spectra in the Soret band of H2TMPyP bound to various synthetic polynucleotides, Biophysical Chemistry 92 (2001) 35–45.
[36] J. Nový, M. Urbanová, Vibrational and electronic circular dichroism study of the interactions of cationic porphyrins with (dG-dC)10 and (dA-dT)10, Biopolymers 85 (2007) 349–358.
[37] X. Chen, M. Liu, Induced chirality of binary aggregates of opposite charged water-soluble porphyrins on DNA matrix, Journal of Inorganic Chemistry 94 (2003) 106–113.
[38] G. Csik, M. Egyeki, L. Herenyi, Z. Majer, K. Toth, Role of structure-proteins in the porphyrin–DNA interaction, Journal of Photochemistry and Photobiology B: Biology 96 (2009) 207–215.
[39] J. Nuno Silva, J. Haigle, J.P.C. Tomé, M.G.P.M.S. Neves, A.C. Tomé, J.-C. Mazière, C. Mazière, R. Santus, J.A.S. Cavaleiro, P. Filipe, P. Morlière, Enhancement of the photodynamic activity of tri-cationic porphyrins towards proliferating keratinocytes by conjugation to poly-S-lysine, Photochemical and Photobiological Sciences 5 (2006) 126–133.
[40] M. Sibrian-Vazquez, T.J. Jensen, F.R. Fronczek, R.P. Hammer, M.G.H. Vicente, Synthesis and characterization of positively charged porphyrin–peptide conjugates, Bioconjugate Chemistry 16 (2005) 852–863.
[41] L. Chaloin, P. Bigey, C. Loup, M. Marin, N. Galeotti, M. Piechaczyk, F. Heitz, B. Meunier, Improvement of porphyrin cellular delivery and activity by conjugation to a carrier peptide, Bioconjugate Chemistry 12 (2001) 691–700.

[42] P. Dozzo, M.-S. Koo, S. Berger, T.M. Forte, S.B. Kahl, Synthesis, characterization, and plasma lipoprotein association of a nucleus-targeted boronated porphyrin, Journal of Medicinal Chemistry 48 (2005) 357–359.
[43] J.M. Kelly, M.J. Murphy, D.J. McConnell, C. Uigin, A comparative study of the interaction of 5,10,15,20-tetrakis(N-methylpyridinium-4-yl)porphyrin and its zinc complex with DNA using fluorescence spectroscopy and topoisomerisation, Nucleic Acids Research 13 (1985) 167–184.
[44] J.B. Le Pecq, J. Paoletti, A fluorescent complex between ethidium bromide and nucleic acids, Journal of Molecular Biology 27 (1967) 87–106.
[45] I. Lubitz, N. Borovok, A. Kotlyar, Interaction of monomolecular G4-DNA nanowires with TMPyP: evidence for intercalation, Biochemistry 46 (2007) 12925–12929.
[46] G. Viola, F. Dall'Acqua, N. Gabellini, S. Moro, D. Vedaldi, H. Ihmels, Indolo [2,3-b]-quinolizinium bromide: an efficient intercalator with DNA-photodamaging properties, ChemBioChem 3 (2002) 550–558.
[47] K.-M. Hyun, S.-D. Choi, S. Lee, S.K. Kim, Can energy transfer be an indicator for DNA intercalation? BBA - General Subjects 1334 (1997) 312–316.
[48] S. Mohammadi, M. Perree-Fauvet, N. Gresh, K. Hillairet, E. Taillandier, Joint molecular modeling and spectroscopic studies of DNA complexes of a bis(arginyl) conjugate of a tricationic porphyrin designed to target the major groove, Biochemistry 37 (1998) 6165–6178.
[49] A.B. Guliaev, N.B. Leontis, Cationic 5,10,15,20-tetrakis (N-methylpyridinium-4-yl) porphyrin fully intercalates at 5′-CG-3′ steps of duplex DNA in solution, Biochemistry 47 (1999) 15425–15437.
[50] A. Harada, K. Shiotsuki, H. Fukushima, H. Yamaguchi, M. Kamachi, Supramolecular assembly of porphyrins and monoclonal antibodies, Inorganic Chemistry 34 (1995) 1070–1076.
[51] K. Toth, J. Bolard, G. Ronto, D. Aslanian, UV-induced small structural changes in the T7 bacteriophage studied by melting methods, Biophysics of Structure and Mechanism 10 (1984) 229–239.
[52] J.-L. Mergny, L. Lacroix, UV melting of G-quadruplexes, Current Protocols in Nucleic Acid Chemistry 17 (Suppl. 37) (2009) 1–15, (unit 17.1).
[53] A. Slama-Schwok, J.-M. Lehn, Interaction of a porphyrin-containing macrotetracyclic receptor molecule with single-stranded and double-stranded polynucleotides. A photophysical study, Biochemistry 29 (1990) 7895–7903.
[54] W.D. Wilson, L. Ratmeyer, M. Zhao, L. Strekowski, D. Boykin, The search for structure-specific nucleic acid-interactive drugs: effects of compound structure on RNA versus DNA interaction strength, Biochemistry 32 (1993) 4098–4104.
[55] S. Frau, E.V. Bichenkova, O.S. Fedorova, S. Lokhov, K.T. Douglas, Binding of a porphyrin conjugate of Hoechst 33258 to DNA. I. UV-visible and melting studies detect multiple binding modes to a 12-mer nonself-complementary duplex, Nucleosides, Nucleotides & Nucleic Acids 20 (2001) 131–143.
[56] M.T. Bjorndal, D. Kuchnir Fygenson, DNA melting in the presence of fluorescent intercalating oxazole yellow dyes measured with a gel-based assay, Biopolymers 65 (2002) 40–44.
[57] K. Andrews, D.R. McMillin, A pared-down version of 5,10,15,20-Tetra(N-methylpyridinium-4-yl)porphyrin intercalates into B-form DNA regardless of base composition: Binding studies of Tri(Nmethylpyridinium4yl)porphyrins, Biochemistry 47 (2008) 1117–1125.
[58] S. Wu, Z. Li, L.G. Ren, B. Chen, F. Liang, X. Zhou, T. Jia, X.P. Cao, Dicationic pyridium porphyrins appending different peripheral substituents: synthesis and studies for their interactions with DNA, Bioorganic & Medicinal Chemistry 14 (2006) 2956–2965.